

Chapter 6

Use of equilibrium and nonequilibrium molecular dynamics to determine solid-liquid phase coexistence at equilibrium

6.1. Introduction

It is often difficult to determine the solid-liquid transition by conventional simulation techniques because of the computational challenges posed by two dense phases. Hansen and Verlet [Han69] reported the first molecular simulation results for solid-liquid phase coexistence. They used a thermodynamic integration algorithm that involves the accurate evaluation of free energies. The widely used Gibbs ensemble simulation algorithm [Pan87] has proven to be a successful technique to determine vapor-liquid and liquid-liquid phase equilibria. However, it is of limited usefulness for solid-liquid phase equilibria, because it is difficult to insert particles into the solid phase. This limitation has been overcome by the Gibbs-Duhem integration technique [Kof93, Agr95] which does not require particle insertions to determine solid-liquid phase equilibria. But the main disadvantage of Gibbs-Duhem integration is that it requires prior knowledge of at least one pair of coexistence points to start the algorithm. The success in predicting the phase boundary largely depends on the accuracy of this starting point.

Nonequilibrium molecular dynamics (NEMD) simulation has proven to be a powerful technique in studying the transport phenomena of liquids [Eva90]. Traditionally, NEMD is mainly confined to the liquid phase. In this chapter we demonstrate that the NEMD technique, in conjunction with standard (NVT) equilibrium MD, can be used to determine the solid-liquid phase coexistence at equilibrium.

This work stems from the insights gained from the work described in Chapter 5 that demonstrated that the pressure and energy of a shearing simple liquid can be expressed in terms of $\dot{\gamma}^\alpha$, where α can be determined at any temperature and density from a simple linear relationship (see Eqn. 5.19).

In this chapter, we show how to estimate the solid-liquid phase transition by this method. We furthermore demonstrate that the imposition of a small strain rate can greatly aid the transition from solid to liquid phases, and show how this method may be used for accurate determination of the solid-liquid phase transition at equilibrium, and how the melting and freezing curves can be efficiently and accurately computed. Both these methods provide alternatives to thermodynamic integration [Han69], Gibbs ensemble [Pan87] and Gibbs-Duhem [Kof93, Agr95] algorithms. Comparison of our results to those in the literature indicates that there is very good agreement. The results also verify our previous observation in Chapter 5 (Eqn. 5.19) that the scaling exponent is a continuous function of temperature and density, and should not be assumed to have the predicted mode-coupling theory value of 3/2.

6.2. Simulation Method

Homogeneous NEMD simulations were performed using the standard SLLOD equations of motion [Eva90], the details of which may be found in Chapters 4 and 5. A Gaussian thermostat is used to constrain the kinetic temperature. Simulation run lengths varied according to the state point requirements. At low density we needed long runs for good statistics, and simulations consisted typically of trajectories of 400000τ , where $\tau = 0.001$ is the time step. Averages of all quantities are then taken over 30-40 trajectories of this length. For high densities this could be reduced to ~ 10 trajectories of 200000τ each while still preserving the same level of statistical accuracy. In all figures presented, error bars represent the standard error unless otherwise stated.

As previously noted, we do not assume any value of the exponent in the pressure (e.g., $3/2$ or 2), but determine its value *a-priori* via a least-squares fit of the pressure as a function of strain rate, based on Eqn (5.19). The pressure we calculate is the hydrostatic pressure, given as one-third the trace of the pressure tensor, which is itself calculated by the standard Irving-Kirkwood expression for a homogeneous nonequilibrium liquid [Irv50]. We then extract the value of α for each (ρ, T) state point, where for each state point we probe the range $0 \leq \dot{\gamma} \leq 0.6$ in steps of 0.1 reduced strain rate units. All our simulations were performed at a potential cut-off radius of 3.5σ .

6.3. Determination of the Equilibrium Solid-Liquid Phase Boundary

6.3.1. Melting Transition

We performed NEMD simulations at three temperatures in the dense liquid phase region according to Figure 6.1. Figure 6.1 illustrates the regions of both vapour-liquid (obtained by Gibbs ensemble simulation) and liquid-solid equilibria obtained for the Lennard-Jones intermolecular potential. For liquid-solid equilibria, literature data obtained from both thermodynamic integration [Han69] and Gibbs-Duhem calculations [Kof93, Agr95] are illustrated. A comparison with our results is also given, the details of which are discussed below. In Figure 6.1, we can identify the melting transition at which the solid phase separates into a two-phase liquid/solid region and a freezing transition at which the single liquid phase is transformed into a two-phase solid/liquid region. In this section, we discuss the simulation of the melting transition.

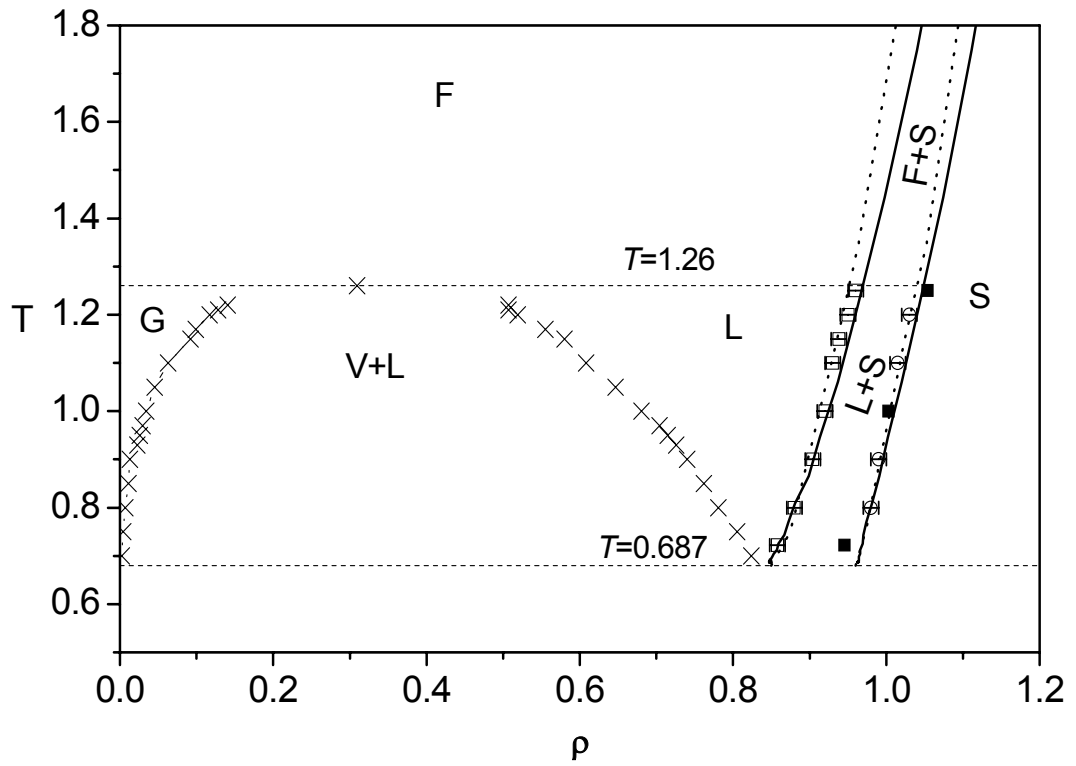


Figure 6.1 Phase diagram of the Lennard-Jones liquid determined by Gibbs ensemble (crosses) and NEMD (open and filled squares and open circles) simulations. Solid lines are data from Kofke [Kof93, Agr95], and dotted lines are data from Hansen and Verlet [Han69].

Figure 6.2 illustrates NEMD simulation results for the high density Lennard-Jones liquid at three temperatures. The significant feature of the results is that at constant temperature a linear relationship is valid over the entire range of liquid densities considered, as indicated by Eqn (5.20). As Eqn (5.20) is the equation of a plane in thermodynamic state-space it is to be expected that the lines at different temperatures are parallel to each other. We note that when the system density is close to the solid-liquid phase boundary the system's pressure becomes unstable. After an initial equilibrium simulation of several tens of thousands of time steps, the time averaged system pressure remains in a value much lower than that of the corresponding equilibrium state after a run of several million time steps. This is an indication that the system is in the close vicinity of the melting transition,

wherein in the former case the system is more solid-like compared to the latter liquid-like state. We further find that within the solid-liquid phase envelope, at any density and non-zero strain rate, the system will reach a nonequilibrium steady-state relatively quickly, after only several thousand time steps.

We have tested the effect of applied strain rate on the time taken to reach a nonequilibrium steady-state and found that this occurs at about 20000 time steps for a strain rate of 0.01. Figure 6.3 shows the comparison of the effect of small strain rates on the steady-state relaxation time for systems at density of 0.92 and 0.96, and $T = 1.00$. Even for the system with density 0.96 (close to the melting transition) at the smallest strain rate of 0.001 only around 170,000 time steps are needed to attain steady-state. This compares very favourably to an equilibrium simulation with no shear, in which millions more time steps are needed to equilibrate within the two-phase liquid/solid region.

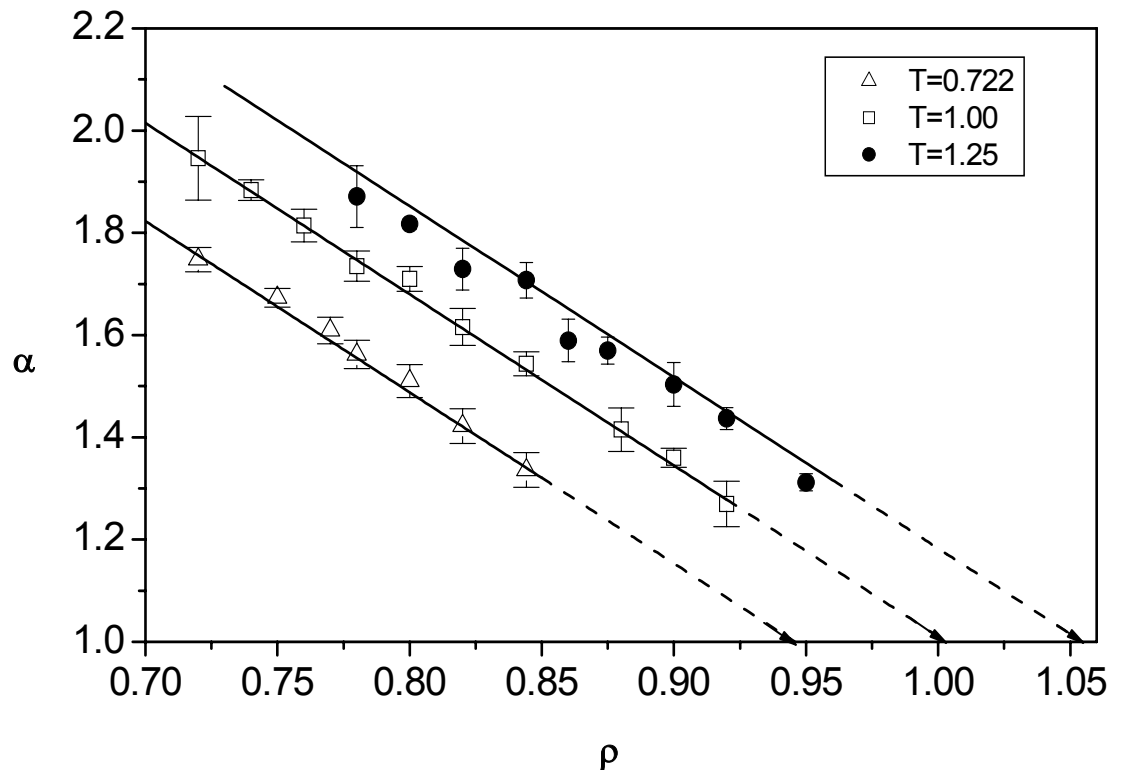


Figure 6.2 α as a function of system density at three temperatures in the liquid region. The symbols represent simulation data (open triangles, $T = 0.722$; open squares, $T = 1.00$; filled circles, $T = 1.25$). The straight lines are linear fits to the data based upon the coefficients of Eqn (5.20), and the arrows represent extrapolation to $\alpha = 1.0$.

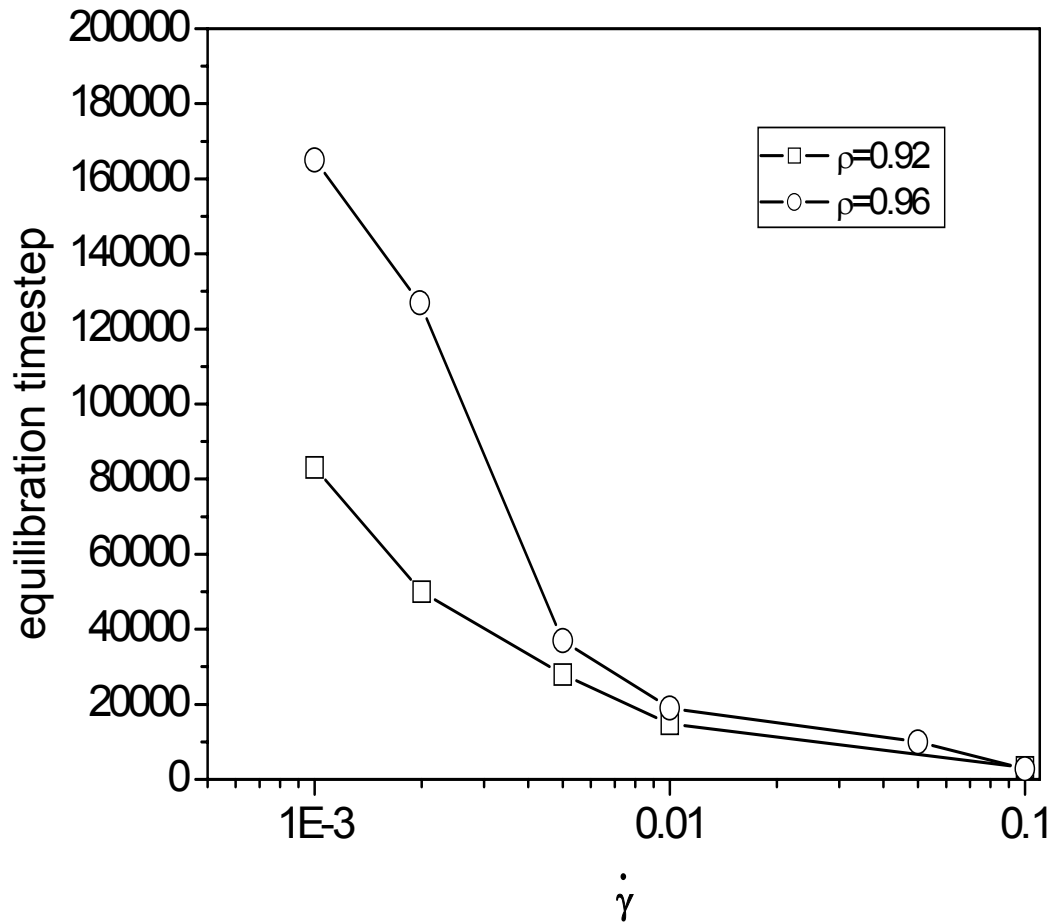


Figure 6.3 The effect of shear rate on equilibration of the dense system at $T = 1.00$.

Figure 6.4 shows the effect of strain rate on time taken for the pressure to relax to its nonequilibrium steady-state value. All runs start at the same face centred cubic (fcc) lattice configuration. A timestep of 0.001 is used. The system density and temperature are 0.96 and 1.0 respectively. It is well known that the time taken to reach steady-state decreases with increasing strain rate [Mor87], and this is clearly observed. The important feature of Figure 6.4, and what makes it useful for our purposes, is that even a very weak strain rate is sufficient to enhance the melting of the crystal. This is particularly useful as we are

interested in the solid-liquid phase transition. After about 170000 time steps the crystal has melted for even the weakest field strength of $\dot{\gamma} = 0.001$. This is evidenced by the increase in pressure in going from the solid to the solid-liquid two-phase region. Contrast this to the bottom curve on Figure 6.4, which is the system pressure with no shear, i.e., at equilibrium. After 170000 time steps the solid has still not melted. We conducted simulations up to 2 million time steps at equilibrium and melting had still not occurred. In general, only after many millions of time steps would melting occur for the equilibrium (i.e., no shear) system.

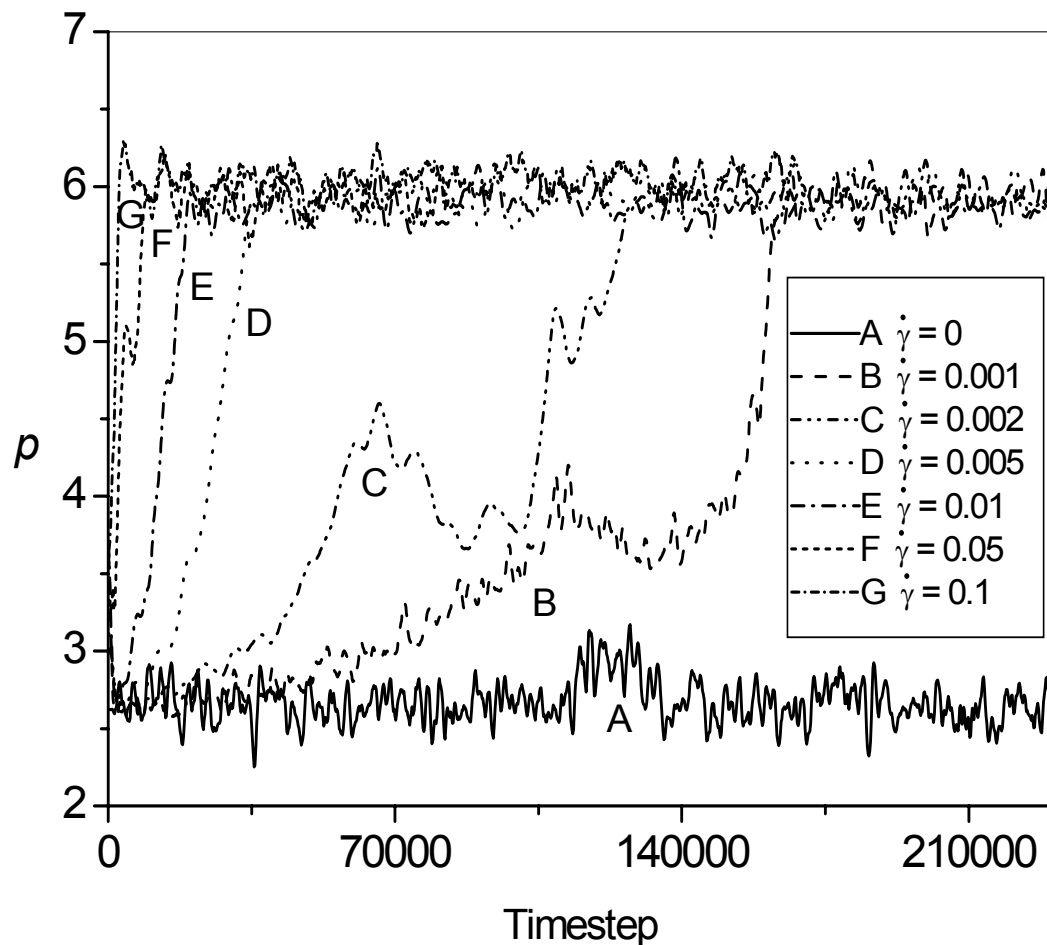


Figure 6.4 Pressure as a function of time step at a density of 0.96 and temperature 1.0. Simulations start from an fcc lattice configuration.

The dynamical behavior at weak non-zero shear rates encourages us to consider the possibility of using NEMD to investigate the melting transition. In the high density two-phase region it is a computationally intensive task to get the melting and freezing points by standard equilibrium techniques. However, with the help of a small strain rate the equilibration process is significantly speeded up, saving a considerable amount of simulation time. If we wish to return to an equilibrium state, we can switch the field off once the solid has yielded and steady-state has been attained. This does not result in the liquid freezing back into the solid phase. This is demonstrated in Figure 6.5. For example, for the weakest strain rate of $\dot{\gamma} = 0.001$ an initial fcc lattice is sheared for 170000 time steps, at which point the solid has yielded and the resulting liquid has reached steady-state. The field is then switched off at $t = 250000\tau$ and the liquid allowed to relax to equilibrium for a further 2 million time steps (we only show times up to 450000τ in Figure 6.5). The difference in pressure between the nonequilibrium steady-state and the final equilibrium liquid state is very small, difficult to observe visually from the plot at the field strengths probed here, and reflects only the structural effects of the shear. Clearly, the liquid has not re-solidified, which would result in a significant pressure drop.

In the liquid-solid two phase region and within our simulation length, after switching off the shear force, we did not observe a glass state at which the pressure of the system is between the liquid branch and the solid branch. We are not sure whether this would happen if the simulation length is much longer. At a density larger than melting density, the glass state did appear. Obviously, the larger the density, the shorter the time needed for the system to become a glass. If we want to obtain the liquid branch pressure and avoid the glass state, we can use nonequilibrium molecular dynamics and the extrapolation method. We can use some different strain rate $\dot{\gamma} \neq 0$, get the pressure vs. strain rate plot, then extrapolate to zero strain rate.

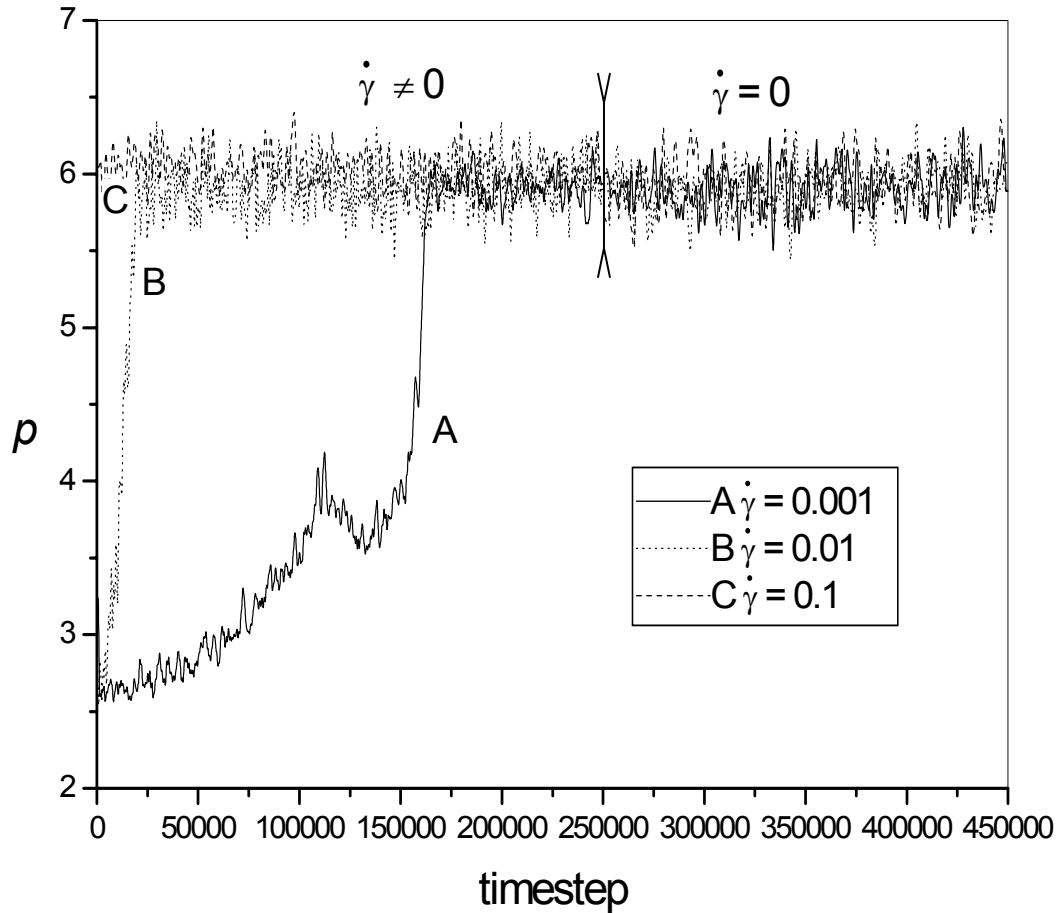


Figure 6.5 Pressure vs. time step for an initial fcc lattice perturbed by a constant strain rate for several different strain rates. The field is then switched off after a time of $t = 250000\tau$ and the liquid allowed to relax to equilibrium.

We ask, can we use NEMD techniques to predict the equilibrium (i.e., zero-shear) melting transition? By examining Figure 6.2 in conjunction with Eqn (5.20), it is apparent that the exponent in the strain rate, α , decreases with increasing density at constant temperature. Significantly, it turns out that at a value of $\alpha = 1.0$ the predicted density is very close to that of the melting transition. At this stage we do not propose a theoretical justification for this, and the value of $\alpha = 1.0$ is based purely on observation. As a demonstration of this phenomenon, let us extrapolate the three lines in Figure 6.2 to the value of $\alpha = 1.0$. Recall

that each line represents the variation of α as a function of density for a constant temperature. At $\alpha = 1.0$ the lines intersect the x -axis and we can easily read off three densities. After performing a simple (NVT) equilibrium molecular dynamics simulation, the system pressure at each interpolated density can be obtained. These three solid phase densities are shown in Figure 6.1, and are depicted by filled squares. They sit on or close to the melting transition curve and are in very good agreement with the calculations reported in the literature [Han69, Kof93, Agr95], as can also be seen in Table 6.1. We also make the observation that liquid-like behaviour is observed for values of $\alpha > 1$, whereas solid-like behaviour is observed for $\alpha \leq 1$.

Table 6.1 Comparison of melting densities, obtained by Hansen and Verlet [Han69], Kofke [Kof93, Agr95], and the present work.

Temperature	Reference [Han69]	Reference [Kof93, Agr95]	Present work
0.722	0.968	0.968	0.946
1.00	1.007	1.012	1.003
1.25	1.037	1.049	1.054

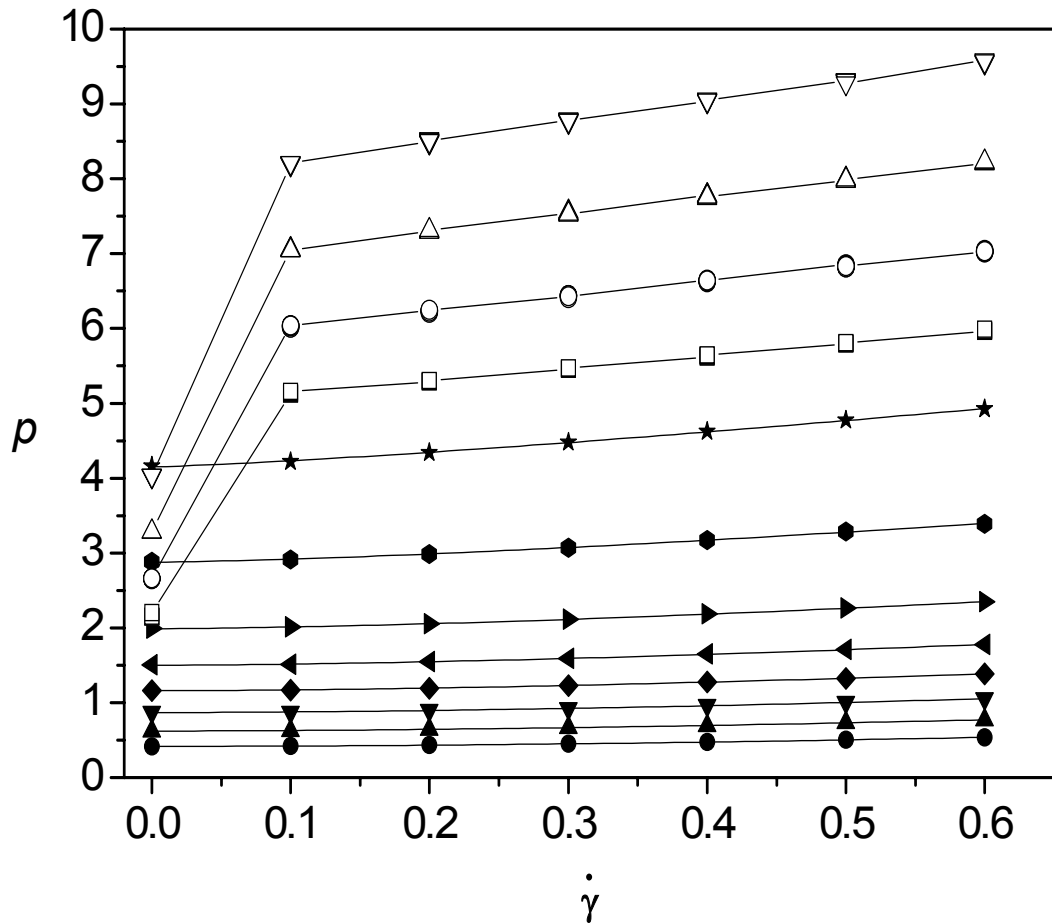


Figure 6.6 Pressure as a function of strain rate at different densities and constant temperature $T = 1.00$. Entry into the two-phase liquid-solid region is clearly seen at higher densities (open symbols) by the sudden drop in pressure at zero strain rate. Filled symbols represent liquid phase densities. The densities from bottom to top curves are, 0.74, 0.76, 0.78, 0.80, 0.82, 0.8442, 0.88, 0.92, 0.94, 0.96, 0.98 and 1.0 respectively.

Figure 6.6 depicts the results of pressure with varying strain rate at $T = 1.00$ and a number of densities. At lower densities the data points are well represented by curves of varying exponent α , as suggested by Eqn (5.20). However, at higher densities the upper four curves show a significantly different feature. At $\dot{\gamma} = 0$ the pressures are even lower than those corresponding to lower densities. This is because at these densities we are in the two-phase liquid-solid region of the phase diagram. When the strain rate is switched on the solid yields and the pressure jumps up suddenly and keeps almost linear with increasing $\dot{\gamma}$. As seen by a comparison with Figures 6.1 and 6.2, a value of $\alpha = 1.0$ gives us the approximate density at the solid line. In order to obtain the approximate density of the solid line at any given temperature, simply set $\alpha = 1.0$ in Eqn (5.20), i.e.,

$$\rho = \frac{A + BT - 1}{C} \quad (6.1)$$

In the case of $T = 1.00$, this gives a value of $\rho = 1.00$ to two significant digits.

There is a limitation to this method. Eqn (6.1) is linear, which means that the predicted solid line can only have a linear form. Clearly this is not the case in general, and is not the case in Figure 6.1. However, Eqn (6.1) is based upon coefficients that were determined only from data obtained within the liquid region of the phase diagram [Ge03]. Thus, within the temperatures spanned by this region ($0.687 \leq T \leq 1.26$) Eqn (6.1) approximates the true solid curve by a line. This limitation could be removed if it was known exactly what the extrapolated value of α is at the solid phase transition. In this work we only assume an approximate value of $\alpha = 1.0$, based upon observation. There is no theory available at present that predicts an accurate or reliable value of α . It is likely that at the solid phase transition the value of α is not a constant value of 1.0 for all values of temperature and density, but varies slightly as functions of these phase variables. Thus, a more accurate melting curve can result.

There is another more accurate and efficient NEMD method we can use to determine the melting transition, and this is indicated by the hollow circle data in Figure 6.1. This data

does not depend on any limiting assumptions made on the value of α . We will discuss how this data is obtained after the following section, in which the underlying principles are discussed.

6.3.2. Freezing Transition

The preceding considerations indicate how the boundary between the single solid phase and the two-phase liquid/solid region (the melting transition) was determined. To complete the phase envelope, we must also determine the boundary between the single liquid phase and the two-phase liquid/solid region (the freezing transition). The procedure for obtaining the densities and pressures for the freezing transition is illustrated with the aid of Figure 6.7 which represents the pressure-density isotherm at a constant temperature of $T = 1.00$.

The pressure-density isotherm is constructed using equilibrium pressures from Gibbs ensemble Monte Carlo (GEMC), (NVT) equilibrium MD and NEMD simulations. In Figure 6.7, the filled squares are data from GEMC simulations, and the crosses represent data from (NVT) MD simulations in the gas phase. The gap between the two densities of vapor-liquid phase equilibrium is the normal two-phase region. Open diamonds represent the dense liquid phase that is obtained by normal (NVT) MD simulations, while the crossed open diamonds represent the two-phase region, obtained by NEMD simulation (discussed below). Open circles depict data for the solid phase, again obtained by equilibrium (NVT) MD simulation. The curve is only used as auxiliary evidence to demonstrate that the solid phase density prediction for the freezing transition is correct. As shown in Figure 6.7 by the filled triangle, the pressure at the density observed at $\alpha = 1.0$ matches the pressure at the freezing density perfectly at this temperature. We point out that the pressure is obtained by equilibrium (NVT) MD simulations at the predicted value of the density, obtained by setting $\alpha = 1.0$.

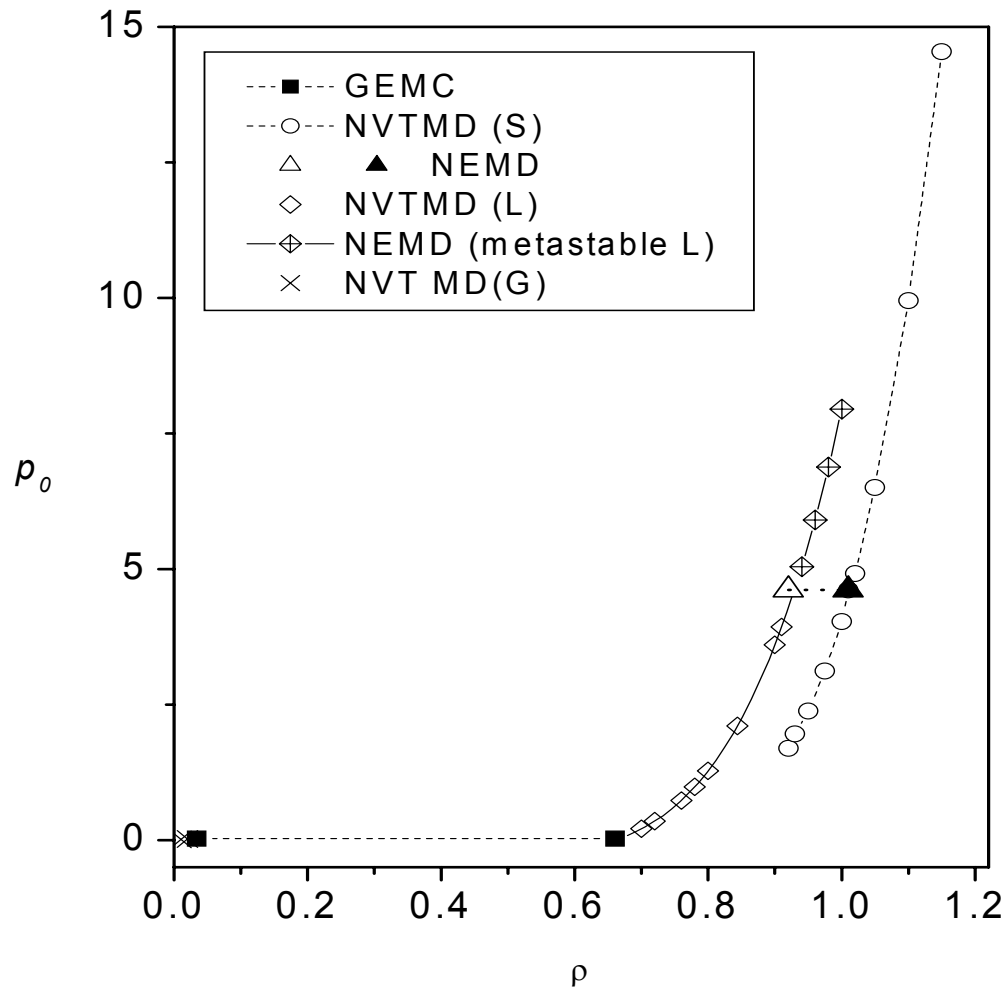


Figure 6.7 Pressure as a function of density at $T = 1.00$. Two phase transition regions are clearly visible. The vapour-liquid equilibria is computed by Gibbs ensemble (GEMC) simulation and the solid-liquid transition is determined by our NEMD method (open and filled triangles). Crosses at low density represent equilibrium (NVT) MD simulation data. Open diamonds represent the liquid phase obtained by equilibrium (NVT) MD simulation, while crossed open diamonds represent the two-phase region obtained by NEMD simulation. Open circles represent the solid branch, again obtained by equilibrium (NVT) MD. Beyond the solid-liquid phase transition point, extension of the solid branch indicates the superheated solid. The symbols G, L and S refer to gas, liquid and solid, respectively.

There are two NEMD methods we can use to obtain the freezing transition. The first method relies upon our knowledge of Eqn (5.20) and that when $\alpha = 1.0$ we are in the solid phase, as discussed earlier. It also requires us to perform equilibrium (*NVT*) MD simulations in the liquid region only. By determining the liquid densities and pressures, we can plot a pressure-density curve for the liquid branch, such as in Figure 6.7 (open diamonds). As discussed above, for a given temperature we can calculate the melting transition density via our NEMD method of approximating the exponent to $\alpha = 1.0$ via Eqn (6.1). We then run an equilibrium (*NVT*) MD simulation to obtain the pressure and plot the density/pressure point in Figure 6.7 (filled triangle). One then draws a tie-line from that point running horizontally along an isobar until it intersects the freezing curve (open triangle in Figure 6.7). The corresponding density at the point of intersection is the liquid phase density of the two-phase liquid/solid boundary, which may then be plotted along with the corresponding temperature on the phase diagram, such as in Figure 6.1.

An alternative and more direct method which combines equilibrium MD and NEMD simulations, and one that does not rely upon the assumption that $\alpha = 1$ in the solid phase, utilizes the fact that a small strain rate applied to the system disturbs its two-phase state. We can see this clearly by again referring to Figure 6.6. In these results, each simulation starts from an initial fcc lattice configuration. The system is allowed to relax to equilibrium ($\dot{\gamma}=0$ simulation) or reach a nonequilibrium steady state ($\dot{\gamma}\neq 0$). At lower liquid densities the pressure follows the simple power law relationship of Eqn (5.19). At higher densities we enter the two-phase liquid-solid region and there is a sharp drop in pressure at $\dot{\gamma} = 0$. In principle, one could determine this transition by performing only equilibrium MD simulations and noting where this pressure drop occurs. However, this is tedious process and would require many equilibrium MD simulations, each separated in density by a very small incremental amount $\Delta\rho$, and spanning a wide range of densities that encompassed the transition density. Furthermore, one could easily miss the transition point by choosing too large a value of $\Delta\rho$. This can be illustrated by reference to Figure 6.7. If, at densities that span the metastable liquid/solid phase, one computes equilibrium pressures in relatively large steps of $\Delta\rho$ it would be possible to move from the liquid to the solid

branch without noticing any significant difference in the pressure. One might then be deceived into believing one is in the liquid phase, whereas in fact the solid phase has already been entered.

This ambiguity can be eliminated by the aid of NEMD simulations. This is because there is such a sharp and easily distinguishable discontinuity in the pressure vs. strain rate curves when the two-phase liquid/solid freezing transition has been entered, as observed in Figure 6.6. In fact, all one needs is just one non-zero strain rate point in addition to the zero strain rate point to see this (e.g., $\dot{\gamma} = 0, 0.1$). If, for each state point, we perform simulations at $\dot{\gamma} = 0, 0.1$, we can easily judge whether we are in the single liquid phase or the two-phase metastable or solid phase by observing the difference in pressure between these two strain rates. If there is a large discontinuity in the pressure, the system is either in the two-phase metastable or solid phase; if there is a small difference in pressure then the system is in the single liquid phase (see Figure 6.6). This allows one to initially coarsely sample a wide range of densities quickly, saving considerable excess simulation time. Once it is clear whereabouts the transition density is it is a simple matter of fine-tuning. Starting in the liquid phase and increasing the density in incremental amounts of $\Delta\rho$, in the limit as $\Delta\rho \rightarrow 0$ the density at which we first observe this discontinuity of the pressure vs. strain rate curve corresponds to the density of the freezing curve of the equilibrium phase diagram in Figure 6.1. Note that this is accurate to within $\Delta\rho$. We plot these results as open squares on the two-phase curve in Figure 6.1, where the horizontal error bars indicate the value of $\Delta\rho$. Very good agreement is found with our method and corresponding results in the literature [Han96, Kof93, Agr95]. It is of interest to note that our results are in better agreement with the results obtained from thermodynamic integration [Han96] than those obtained from the Gibbs-Duhem algorithm [Kof93, Agr95]. This may possibly reflect the influence of the choice of starting point used for the Gibbs-Duhem calculations, or different cut-off conditions in the different reported simulations.

We note here that this method is extremely efficient in obtaining the metastable points, and was used to calculate these in Figure 6.7 (crossed open diamond symbols). One cannot easily obtain metastable points by conventional Monte Carlo or equilibrium molecular

dynamics simulations in the two-phase region due to the long simulation times required. However, the application of a very small strain rate can easily force the solid to yield, thus breaking the crystalline structure of a starting fcc lattice to reach the metastable phase. After the system reaches a nonequilibrium steady state, we switch off the field and continue an equilibrium MD simulation using as input the configuration obtained from the NEMD simulation. Or, we can conduct NEMD simulations using several strain rates at the same state point. We can then obtain the relevant quantities at equilibrium by extrapolating to zero field. The latter method is useful when one deals with high density points. For these state points, we can add a field to melt the crystal with ease. But after switching off the field, the system can only stay on the liquid branch for a short time and then begins to freeze back into a solid. The alternative standard way to calculate the two-phase region is by condensing or quenching the system at very slow rates [Ber83], which takes considerably more CPU time.

Our work differs to that recently reported by Butler and Harrowell [But02, But03], who examined the coexistence between a strained crystal and its shearing melt. While their work focused on the coexistence away from equilibrium using inhomogeneous methods (i.e., physical modelling of the walls, and moving them to simulate planar Couette flow), our work applies the standard homogeneous NEMD algorithm (i.e., SLLOD [Eva90]) to determine the equilibrium coexistence of the solid-liquid phase transition.

6.3.3. Melting Transition Revisited

Once the freezing point has been determined (section 6.3.2), it is relatively straightforward to determine the melting point. As discussed in section 6.3.2 and illustrated in Figure 6.7, at any temperature the liquid branch of the isothermal curve and its metastable extension can be easily calculated from NEMD. For any freezing point on the liquid branch, extending an isobaric tie line from the liquid branch onto the solid branch can identify the melting point on this curve. The point of intersection with the solid branch gives the corresponding density of the melting transition. This data is shown in Figure 6.1 as hollow circles, where again the error in density corresponds to $\Delta\rho$, as discussed before. Excellent agreement is found between our data and that of previous workers [Han96, Ko93, Agr95].

Again we note that our data agrees better with thermodynamic integration results [Han96] than the Gibbs-Duhem data [Kof93, Agr95].

6.3.4. Comparison with other algorithms

It is of interest to compare our procedure with the alternative methods for obtaining solid-liquid phase coexistence. Thermodynamic integration is arguably the least routine method because it requires accurate values of free energies that are difficult to obtain. In principle, the Gibbs ensemble could be applied to obtain solid-liquid equilibria. However, the low probability of exchanging particles between the dense liquid and solid phases means that it is not a practical option in most cases. Gibbs-Duhem integration is the most computationally efficient method but it suffers from the disadvantage that it is not self-starting, requiring knowledge of one coexistence point. The accuracy of the Gibbs-Duhem method critically depends on this initial starting point. We note that recently [Cha03] a new algorithm for solid-liquid equilibria has been proposed which uses histogram reweighting techniques to overcome this limitation.

In common with the Gibbs-Duhem method, our procedures have the advantage that they do not involve particle insertions. In addition, they have the further advantage that they do not require an initial starting point and the solid-liquid phase envelope can be determined entirely *a-priori*. Our method of determining the melting transition by setting $\alpha = 1$ does have a limitation at present in that it can only approximate the solid phase transition curve as a line. It is hoped that this limitation will be removed once a theoretical determination of the exact value of α at the solid phase transition is obtained. Even without this knowledge, this method is a useful tool that can be used to estimate the melting curve. Our alternative method of determining both the two-phase solid-liquid freezing and melting coexistence curves by applying a small strain rate to yield an initial crystal configuration is completely general and suffers from no such limitation. It is both accurate and computationally efficient.

6.4. Conclusions

We have computed the melting and freezing curves for an equilibrium Lennard-Jones system of atoms by a combination of equilibrium and nonequilibrium molecular dynamics simulations. One method relies upon our previous discovery that the strain rate power exponent of the pressure is a continuous linear function of temperature and density, and ranges within approximately $1.2 \leq \alpha \leq 2$ in the liquid phase. In this work we demonstrate that the exponent takes on an approximate value of $\alpha = 1.0$ at the solid-liquid melting phase transition. Knowledge of this exponent allows us to predict the melting density at any temperature, and enables us to construct the melting curve. The solid phase density observed is consistent with that of other work [Han96, Kof93, Agr95]. The corresponding freezing curve can also readily be obtained by intercepting a tie line from the solid phase with the isotropic liquid curve. This method is limited by the approximation we necessarily place upon the value of α at the melting phase transition. Further theoretical work is required to extend and validate this approach to other systems.

To overcome this limitation we have used a combination of equilibrium MD and NEMD methods that relies upon no such approximation. By noting that there is a discontinuity in the pressure vs. strain rate curve once the two-phase region is entered, we can quickly and accurately compute both the freezing and melting equilibrium phase transition curves. We note that it is nearly impossible to get the two-phase region by conventional Monte Carlo and equilibrium molecular dynamics simulations starting from an fcc lattice. However, the application of a very small strain rate can easily force the starting crystal to yield and break the crystalline structure to reach the two-phase region.

Finally, we comment that while this series of calculations was performed on the Lennard-Jones liquid, there is no reason why it should not work for other liquids (atomic or molecular) with different potentials that exhibit relatively simple phase diagram. By observing when the solid yields by application of a small shearing field it is straightforward to compute the freezing transition, from which the melting transition can be computed. We

point out that our simulations started from a FCC structure. We have not yet determined if the method is still useful with other initial crystal structures.